Environmental Science & Technology

Article

Cite This: Environ. Sci. Technol. 2019, 53, 9491−9501

pubs.acs.org/est

Field and Laboratory Studies Linking Hydrologic, Geochemical, and Microbiological Processes and Enhanced Denitrification during Infiltration for Managed Recharge

Galen Gorski,[*,†] Andrew T Fisher,[†] Sarah Beganskas,[†,#] Walker B Weir,[†,$] Kaitlyn Redford,[‡,⊥] Calla Schmidt,[§] and Chad Saltikov[‡]

[†]Department of Earth and Planetary Sciences, University of California Santa Cruz, Santa Cruz, California 95064, United States

[‡]Department of Microbiology and Environmental Toxicology, University of California, Santa Cruz, California 95064, United States

[§]Department of Environmental Science, University of San Francisco, San Francisco, California 94117, United States

Supporting Information

ABSTRACT: We present linked field and laboratory studies investigating controls on enhanced nitrate processing during infiltration for managed aquifer recharge. We examine how carbon-rich permeable reactive barriers (PRBs) made of woodchips or biochar, placed in the path of infiltrating water, stimulate microbial denitrification. In field studies with infiltration of 0.2−0.3 m/day and initial nitrate concentrations of $[NO_3\text{-}N]$ = 20−28 mg/L, we observed that woodchips promoted 37 ± 6.6% nitrate removal (primarily via denitrification), and biochar promoted 33 ± 12% nitrate removal (likely via denitrification and physical absorption effects). In contrast, unamended soil at the same site generated <5% denitrification. We find that the presence of a carbon-rich PRB has a modest effect on the underlying soil microbial community structure in these experiments, indicating that existing consortia have the capability to carry out denitrification given favorable conditions. In laboratory studies using intact cores from the same site, we extend the results to quantify how infiltration rate influences denitrification, with and without a carbon-rich PRB. We find that the influence of both PRB materials is diminished at higher infiltration rates (>0.7 m/day) but can still result in denitrification. These results demonstrate a quantitative relationship between infiltration rate and denitrification that depends on the presence and nature of a PRB. Combined results from these field and laboratory experiments, with complementary studies of denitrification during infiltration through other soils, suggest a framework for understanding linked hydrologic and chemical controls on microbial denitrification (and potentially other redox-sensitive processes) that could improve water quality during managed recharge.

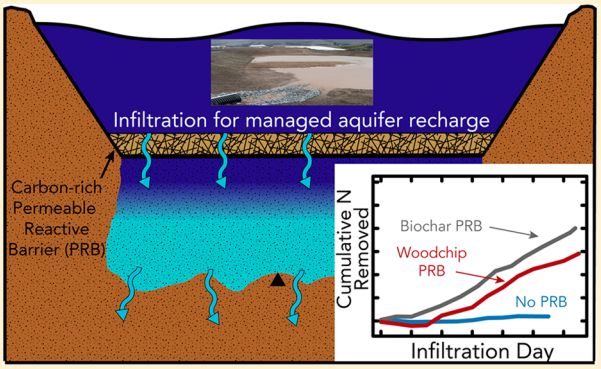

1. INTRODUCTION

Managed aquifer recharge (MAR) is an important technique for sustaining groundwater supplies and mitigating the impact of increased demand, climate change, and shifting land use.[1] MAR projects collect and infiltrate excess surface water flows using a variety of techniques including stream-bank filtration, dry wells, and dedicated infiltration basins.[2] Water for MAR can be derived from nonpristine sources such as stormwater,[3] treated wastewater,[4] or other excess surface flows;[5] in some cases, these source waters can contain contaminants that threaten groundwater quality. In addition, infiltrating water is subject to physical, geochemical, and microbiological processing, which can improve or degrade water quality.[6−10]

Nitrate (NO_3) is a common and pervasive contaminant in both groundwater[11] and surface water,[12,13] and elevated concentrations have been linked to toxicity in humans and negative environmental effects on ecosystems.[14,15] Nitrate can be removed through microbial denitrification,[16] a multistep process that (if run to completion) converts nitrate to inert N_2 gas through a series of reactive intermediates. Denitrification requires an electron donor (often in the form of organic carbon), takes place under suboxic to anoxic conditions, and can be affected by additional factors such as soil pH, temperature, saturation, and vegetation.[17]

Earlier studies have demonstrated the feasibility of enhancing denitrification with carbon-rich permeable reactive barriers (PRBs) made of materials such as woodchips, biochar, or compost.[18,19] These materials are often used in denitrification bioreactors, a broad class of systems designed to reduce nitrate concentrations in agricultural runoff,[20] treated

Received: February 26, 2019
Revised: July 17, 2019
Accepted: July 28, 2019
Published: July 29, 2019

DOI: 10.1021/acs.est.9b01191
Environ. Sci. Technol. 2019, 53, 9491−9501

wastewater,[21] contaminated groundwater,[22] and other settings.[23]

PRBs can be applied in conjunction with MAR to improve water quality during infiltration, particularly by enhancing denitrification. For example, a PRB made of vegetal compost and woodchips was installed in an MAR system to promote denitrification during infiltration of diverted river water, resulting in 30−40% nitrogen removal on some days but negligible removal or addition on other days.[5] Controlled percolation experiments using water with elevated [NO_3] demonstrated that adding a woodchip PRB to coarse-grained soils (>90% sand) led to enhanced denitrification during rapid infiltration.[24] This study also noted a negative correlation between rates of infiltration and denitrification, with tests run at infiltration rates up to 1.9 m/day. While these studies show promise in using a PRB to enhance denitrification during infiltration for MAR, the notable variability in the occurrence and extent of denitrification highlights sensitivity to chemical and hydrologic conditions. This makes it difficult to design and operate MAR systems beyond the specific sets of parameters and conditions documented at each site.

MAR systems operate across a range of soil substrates and fluid chemistries, and understanding the complex interactions between soil characteristics (e.g., grainsize distribution, soil organic matter), hydrologic conditions (e.g., infiltration rate, saturated zone thickness, fluid residence time), and chemical constraints (e.g., abundance and/or availability of electron donors) during infiltration is important for maximizing water quality benefits during MAR and avoiding resource degradation. While a subset of these factors has been investigated (e.g., increased carbon on denitrification in bioreactors), few studies have combined colocated measurements of hydrologic, geochemical, and microbiological data in order to elucidate the fundamental processes that control denitrification at rapid infiltration rates that are typical for MAR systems.

In this study, we present colocated physical, geochemical, and microbiological observations from linked field and laboratory studies using intact soil cores from the same site to quantify how horizontal PRBs made from carbon-rich materials (woodchips or biochar) can enhance denitrification during infiltration for MAR. We are particularly interested in quantifying the dependence of denitrification on infiltration rate with and without a PRB. The field and laboratory studies link hydrologic conditions and the nature of carbon-rich PRB materials to concomitant geochemical and microbiological changes during infiltration. Laboratory studies are particularly useful in this context for extending field results to different flow rates. We present data from new experiments, combine these results with those from other studies, and propose a conceptual framework for understanding denitrification during infiltration leading to MAR, including a dependence on flow rate, with and without a carbon-rich PRB.

2. MATERIALS AND METHODS

2.1. Study Site. The study site for this project was an active ranch in the Pajaro Valley near Watsonville CA, adjacent to Monterey Bay and the Pacific Ocean (Figure S1), where installation of an MAR infiltration system is planned that will collect stormwater runoff from >1000 acres of farmland and rangeland. Soils at the site are representative of soils in the southeastern portion of the valley, comprising mainly flood plain, alluvial, and fluvial deposits adjacent to the Pajaro River, the primary drainage channel for the valley. Other infiltration and recharge projects are being operated nearby or are being considered for installation.[3,25]

2.2. Experimental Design and Operation: Field studies. Field percolation studies emulated continuous infiltration that would occur during MAR operation, using an experimental design similar to that applied in an earlier study of coarser soils in the same region[24] (Figure 1A and SI, Sections S1.2−S1.3). The current study differs from earlier work in several respects, including testing of adjacent materials in the field and lab. Three square plots with an area of 1 m^2 were hand-excavated to 1 m depth. Lateral flow through the sides of the plots was limited by installing fiberglass walls on plot sides, caulking corner joints, and backfilling the annulus around the walls with activated bentonite.

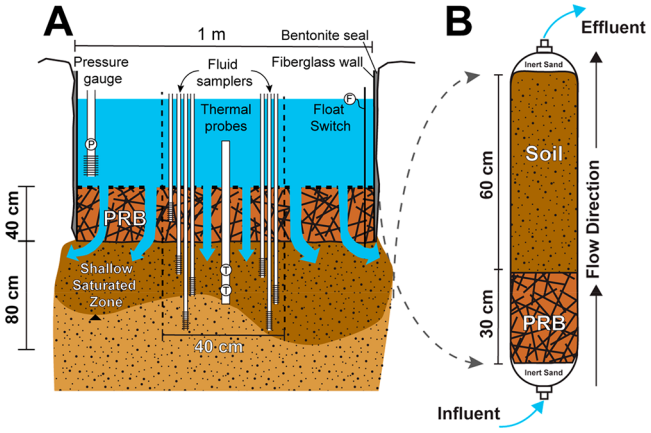

Figure 1. Field and laboratory experimental configurations. (A) Cross section of layout and plot construction for field percolation studies, with instrumentation installed within the central 0.16 m^2 of the plot. PRB layer was installed for tests with woodchips (*WC-Perc*) and biochar (*BC-Perc*). For native soil test *NS-Perc*, the plot construction was identical except no PRB layer was installed. (B) Laboratory column studies were designed to simulate the saturated zone within the field studies with identical layering. Columns were inverted for testing to maintain saturated conditions under different infiltration rates, retaining the same flow direction as used for field tests.

One plot was used as a control to test native soil conditions (*NS-Perc*), and the other two plots were augmented with 40 cm thick PRBs made of woodchips (*WC-Perc*) or biochar (*BC-Perc*), installed above the plot base (see SI, Sections S1.2−S1.4 for details). During each test, water with elevated [NO_3] was applied to the plot through an inlet hose supplied by a nearby groundwater well. Water level was controlled with an automated inflow management system that used a float switch connected to a solenoid valve. The system maintained saturated conditions below the base of the plot and prevented overtopping the plot walls. Tests were run sequentially, each for 14−15 continuous days to establish saturated, quasi-stable conditions in the subsurface below the plot base.

2.3. Physical Hydrology: Field Studies. Infiltration testing generally results in a large fraction of horizontal flow, especially around the edges of the test plot (see discussion in S1.5 for details). Fluid measurement and sampling instrumentation for this study was placed within a 0.4 × 0.4 m central area within each plot, where the vertical component of infiltration was expected to be greatest.

The tests were designed to facilitate independent measurements of total infiltration and the vertical component of

DOI: 10.1021/acs.est.9b01191
Environ. Sci. Technol. 2019, 53, 9491−9501

infiltration near the center of the plot. Total infiltration was measured by recording the change in water stage over time during each infiltration cycle (the period of time when there was no flow into the plot and water was infiltrating into the subsurface). Temperature loggers were installed in thermal probes, at depths of 5 and 20 cm below the base of the plot (bpb), to measure the vertical component of infiltration using heat as a tracer.[26]

2.4. Experimental Design and Operation: Lab Studies. Intact soil cores (60 cm × 10 cm ID) for laboratory testing were collected adjacent to field test locations using a custom hammer coring system (SI, Figure S2 and Section S1.10). After cores were transported to the lab, woodchips, biochar, or coarse sand (1−2 mm, well rounded, ≥ 95% silica, used as a control) was added to the top of the cores as a PRB layer (∼30 cm thick, similar to that used for field testing), and the cores were sealed and inverted for testing. These tests are referred to as *WC-Col*, *BC-Col*, and *NS-Col*, respectively.

A solution of local tap water and NO_3 (∼30 mg/L N-NO_3) was premixed in a 550 L tank and then pumped through the columns in an upward flow direction so that saturated conditions could be maintained across a range of flow rates; this approach has been taken in earlier studies[27−31] (see SI, Section S1.10 for more details). Results from column tests are presented for two analysis periods of quasi-stable flow, AP1 and AP2 (Figure S4). AP1 lasted from infiltration day (ID)-32 to ID-52, when the vertical rate was ∼0.17 m/day, overlapping with vertical infiltration rates observed in the field percolation experiments. The pumping rate was increased to ∼0.72 m/day and flow was allowed to stabilize for 18 days with AP2 occurring from ID-71 to ID-94 (Figure S4).

2.5. Fluid Sampling and Analysis. For field tests, two nests of mini-piezometers (screens 10 cm long) were installed in the soil below each field plot to sample infiltrating fluid, with screened depths centered at 30, 55, and 80 cm bpb (Figure 1A). Another fluid sampler was installed in each plot to sample water before it infiltrated. In *WC-Perc* and *BC-Perc*, an additional fluid sampler was placed within the PRB layer. During laboratory tests, influent and effluent samples were collected from each core. Fluid samples were collected during both percolation and laboratory experiments every 1−2 days.

All fluid samples were analyzed for nitrogen species (NO_3, NO_2, and NH_4) and dissolved organic carbon (DOC). A subset of the field fluid samples was analyzed for $\delta^{15}N$ and $\delta^{18}O$ of NO_3. Analytical methods for these solutes and isotopes are discussed in SI, Section S1.7.

Net changes in solutes for each day were calculated as

$$\Delta[N] = ([NO_3\text{-}N] + [NO_2\text{-}N] + [NH_4\text{-}N])_{depth} - ([NO_3\text{-}N] + [NO_2\text{-}N] + [NH_4\text{-}N])_{surface} \quad (1)$$

$$\Delta[DOC] = [DOC]_{depth} - [DOC]_{surface} \quad (2)$$

where $\Delta[N]$ and $\Delta[DOC]$ are net changes in inorganic nitrogen and DOC concentrations (mg/L). For field studies, *surface* and *depth* refer to the inflowing water and water sampled from the 80 cm piezometer, respectively, unless otherwise stated. For lab studies, *surface* and *depth* refer to the influent and effluent, respectively, corresponding to the same infiltration flow direction as in the field. $\Delta[N]$ accounts for interconversion of N between species but neglects common gaseous forms of N such as NO, N_2O, and N_2, intermediate, and final products of denitrification.

The mass of nitrogen removed from the system as $\Delta[N]$ was converted to a rate of mass loss

$$\Delta N_L = (\Delta[N] \times IR_V) \quad (3)$$

where ΔN_L = load reduction (g-N·m^{-2}·day^{-1}), and $\Delta N_L < 0$ indicates a net removal of nitrogen. IR_V is the vertical infiltration rate for field tests and the measured flow rate for the laboratory studies. We use vertical infiltration rates as these values represent conditions near the center of the plots (where fluid samples were collected and thermal probes were deployed), which allows the most direct comparison between field and lab experiments (see SI, Section S1.5 for more details) and operating conditions during MAR. In order to distinguish differences in $\Delta[N]$ and ΔN_L between experimental treatments and between flow rates, single-tailed t tests were conducted in experimental results. To distinguish differences with depth within experiments, single-factor ANOVA tests were performed. For both tests, results were considered significant when $p < 0.05$.

2.6. Sediment Sampling and Analysis. Sediment samples were collected before and after each field and lab experiment and analyzed for (1) soil texture, (2) total organic carbon (TOC) and total nitrogen (TN), and (3) phylogenetic sequencing of microbial DNA. Microbial samples were collected using sterile techniques and were immediately placed in a liquid nitrogen field dewar for storage. DNA samples were kept at −80 °C until extraction.

2.7. DNA Extraction and Phylogenetic Sequencing. Methods for microbial analysis of soil samples were similar to those applied in an earlier study in the Pajaro Valley.[24] Briefly, soil DNA was extracted with a PowerSoil DNA Isolation Kit (QIAGEN). The Qubit 4 Fluorometer (Invitrogen) was used to quantify DNA extracts. PCT amplicons (∼550 bp) were generated from PCRs with soil DNA and 16S rRNA gene primers targeting the V4 and V5 variable regions. The PCR amplicon sequencing pipeline used in this study was adapted from Illumina MiSeq platform protocol for 16S metagenomic libraries.[24] The overall pipeline included steps for the primary PCR using 16S rRNA primers,[32] PCR cleanup, library preparation (adding unique sequencing indices [barcodes] to each PCR amplicon), normalizing DNA concentrations of each library, and library pooling. The pooled library was sequenced on the Illumina MiSeq (600 cycles v3 PE300 flow cell kit) at the University of California, Davis Genome Center. The raw sequence reads have been uploaded to the National Center for Biotechnology Information Sequence Read Archive (accession number: PRJNA523645).

2.8. Phylogenetic Data Processing. To analyze differences in microbial community structure, soil samples were grouped based on experimental conditions (see supporting tables). Samples were grouped into six categories based on (1) experiment (field or laboratory), (2) treatment (NS, WC, or BC), and (3) whether they were collected before or after infiltration. Within each group, samples collected from 10 and 30 cm depth were grouped and selected for comparison, as these depths showed the most significant nutrient cycling. For more detail, see SI, Section S1.6.

3. RESULTS

3.1. Field Studies. The first 6 days of field percolation tests comprised an "initialization period," when the soil system was

DOI: 10.1021/acs.est.9b01191
Environ. Sci. Technol. 2019, 53, 9491−9501

saturating, and biogeochemical cycling adapted to new storage and flow conditions (Figure 2). During the subsequent

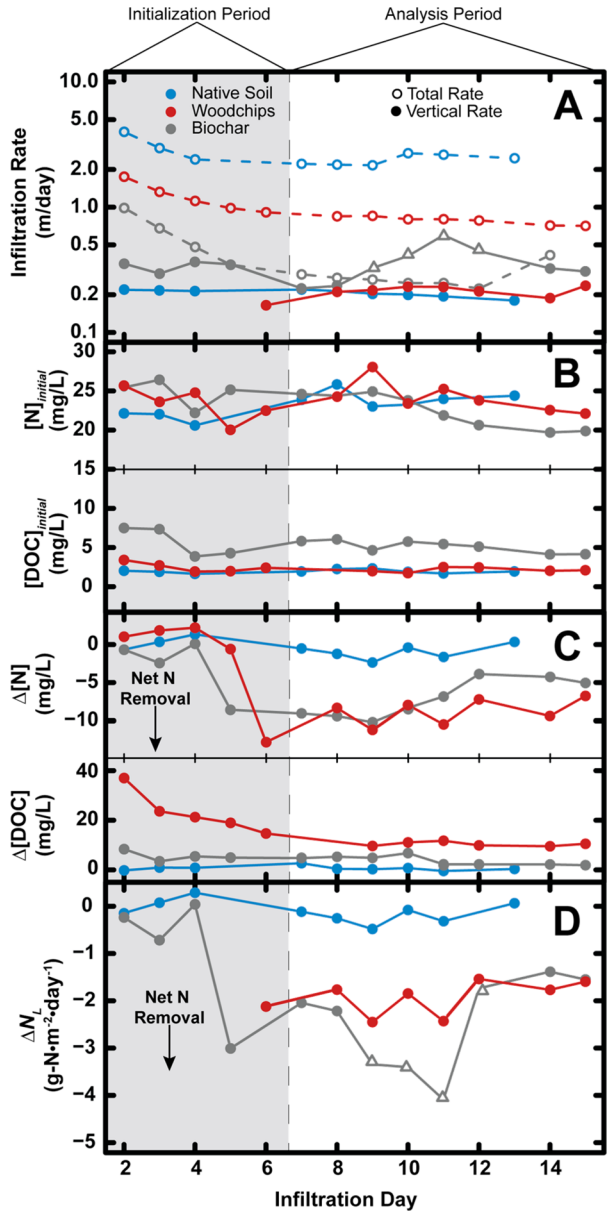

Figure 2. Results from field percolation experiments for three soil treatments showed enhanced nutrient cycling in both *WC-Perc* (red) and *BC-Perc* (gray) compared to *NS-Perc* (blue). Experiments were divided into initialization period (gray) and analysis period (white). (A) Total (open circles with dashed lines) and vertical (closed circles with solid lines) infiltration rates. (B) Surface [*N*] and [DOC]. (C) Δ[*N*] and [DOC] between surface and 80 cm fluid sampler. (D) Daily ΔN_L measurements for each treatment as defined by eq 3. Open triangles in parts A and D indicate the data was not used for ΔN_L calculations; see section on Soils and Infiltration Rates for explanation.

"analysis period", total infiltration rates were relatively stable and nutrient concentrations developed consistent patterns relative to the initialization period.

3.1.1. Soils and Infiltration Rates. Soil samples from the three field plots had median clay, silt, and sand fractions consistent with textural characterization of loam (Figure S5). However, some samples from *NS-Perc* and *WC-Perc* were sandy loam, whereas some samples from *BC-Perc* were finer, particularly in the upper 20 cm bps, including silt loam. All soil samples showed consistent TOC (0.3−0.9%-wt) and TN (0.04−0.08%-wt); there was no systematic variation with depth or soil treatment, and no systematic difference between samples collected before and after the tests (Figures S6 and S7).

Mean total infiltration rates were 2.40, 0.78, and 0.28 m/day for *NS-Perc*, *WC-Perc*, and *BC-Perc*, respectively (Figure 2A). The differences in these infiltration rates are best explained by local soil heterogeneity, as plots were constructed on adjacent areas (separated laterally by 3−4 m), using identical configurations and materials. In addition to differences in soil texture, macropores can lead to large variations in hydraulic properties. Similar spatial differences in infiltration rates have been observed during earlier tests in sandy deposits[24] and in measurements made in active managed recharge systems.[3,33]

Vertical infiltration rates for *NS-Perc* and *WC-Perc* were consistent throughout the experiments (IR_V = 0.20 and 0.21 m/day, respectively) whereas vertical infiltration rates for *BC-Perc* were higher (IR_V = 0.36 m/day) and more variable, peaking near ID-11 (IR_V = 0.60 m/day) and exceeding total infiltration rates for several days (Figure 2A). Vertical infiltration rates are point measurements, whereas total infiltration rates are calculated by mass balance and applied to the full plot area. When vertical infiltration rates exceed total infiltration rates, this likely indicates a response to highly conductive infiltration paths, perhaps root tubules or burrows.[3,34] It is unlikely that water flowed quickly down the side of the probe as the annulus around the thermal probes was filled with silica slurry during installation. Because these transient rates are not representative of broader infiltration conditions and nutrient load is calculated explicitly using the vertical infiltration rate (equation 3), we do not include data from these days (ID-9 to ID-13 in *BC-Perc*) in the assessment of ΔN_L. However, we include a longer infiltration record (ID-7 to ID-15) for analysis of Δ[*N*] and Δ[DOC], as these values are calculated using only the differences between observed concentrations at the surface and at depths.

3.1.2. Nutrient Changes. The water supply for field percolation tests had elevated [NO_3-N] throughout the experiments, ranging from 20 to 28 mg/L (Figure 2B). Variability in the surface concentration resulted from pulling this water from a nearby supply well. Influent [NO_2-N] was below detection in 7 of 21 samples (always ≤0.8 mg/L), and [NH_4-N] was below detection in all influent samples except one (0.1 mg/L; see SI Tables). Pore fluid analyses indicated the smallest systematic shift in [*N*] during *NS-Perc* (Δ[*N*] = −1.0 ± 1.4 mg/L), whereas Δ[*N*] during *WC-Perc* and *BC-Perc* showed greater changes (Δ[*N*] = −8.8 ± 2.5 mg/L and −7.1 ± 3.3 mg/L, respectively; Table 1 and Figure 2C), indicating more nitrate removal ($p < 0.05$). Δ[*N*] was more variable during *BC-Perc*, ranging from −10.2 mg/L on ID-9 to −3.9 mg/L on ID-12, but *WC-Perc* and *BC-Perc* showed statistically similar Δ[*N*] ($p > 0.05$).

WC-Perc showed consistent load reduction, with ΔN_L values between −1.5 and −2.5 g-N·m^{-2}·day^{-1} (Figure 2D), and *BC-Perc* showed ΔN_L values similar to *WC-Perc* ($p > 0.05$), ΔN_L= −2.2 to −1.4 g-N·m^{-2}·day^{-1}. Surface [DOC] was consistent during individual percolation tests but was lower during *NS-Perc* and *WC-Perc* (2.0 and 3.0 mg/L, respectively) than during *BC-Perc* (5.1 mg/L). Δ[DOC] was greatest in *WC-Perc* with an average of 10.4 ± 1.3 mg/L compared to 3.8 ± 3.0 mg/L

DOI: 10.1021/acs.est.9b01191
Environ. Sci. Technol. 2019, 53, 9491−9501

Table 1. Summary of Experimental Conditions and Key Results for All Experiments

Experiment	Treatment	Analysis Period	Total Infiltration Days (n)	Analysis Days[a] (n)	Total Infiltration Rate (m/day)	Vertical Infiltration Rate (m/day)	Surface $[N]$ (mg/L)	Depth[c] $[N]$ (mg/L)	Surface [DOC] (mg/L)	Depth[c] [DOC] (mg/L)	$\Delta[N]$ (mg/L)	ΔN_L (g/day/m^2)
Field	NS	A	13	6	2.40(0.22)	0.20(0.01)	24.1(1.0)	23.1(1.5)	2.0(0.2)	2.7(1.1)	−1.0(1.0)	−0.2(0.2)
Laboratory	NS	AP1	19	12		0.17(0.02)	31.5(0.6)	29.3(0.6)	27.6(1.5)	30.9(2.9)	−2.3(0.9)	−0.4(0.1)
Laboratory	NS	AP2	23	10		0.74(0.03)	31.7(1.3)	31.3(2.2)	30.8(5.5)	30.5(4.7)	−0.4(2.0)	−0.3(1.4)
Field	WC	A	15	7	0.78(0.06)	0.21(0.03)	24.2(2.0)	15.4(1.2)	2.1(1.5)	12.5(1.0)	−8.8(1.7)	−1.9[d](0.4)
Laboratory	WC	AP1	19	12		0.18(0.02)	31.4(0.6)	22.6(0.9)	27.4(1.5)	37.1(3.1)	−8.8[d](0.7)	−1.6[d](0.2)
Laboratory	WC	AP2	23	10		0.70(0.04)	31.7(1.3)	30.2(1.6)	30.6(5.2)	31.5(4.6)	−1.4(1.0)	−1.0(0.7)
Field	BC	A	15	8(4)[b]	0.28(0.06)	0.27(0.05)	22.5(2.2)	15.3(0.7)	5.1(0.8)	8.9(2.4)	−7.1(2.5)	−1.8[d](0.3)
Laboratory	BC	AP1	19	13		0.18(0.02)	31.5(0.6)	26.5(1.0)	27.2(1.9)	31.2(2.5)	−5.0[d](0.8)	−0.9[d](0.2)
Laboratory	BC	AP2	23	11		0.71(0.03)	31.6(1.3)	31.1(1.4)	30.6(5.2)	30.6(5.4)	−0.5(1.4)	−0.4(1.0)

[a]Number of days in which fluid samples were collected during each analysis period. [b]For *BC-Perc*, 8 days (ID-7−ID-15) were used in reported values for Total Infiltration Rate, $[N]$, [DOC], and $\Delta[N]$, but 4 days (ID-7−ID-8 and ID-14−ID-15) were used for analysis of Vertical Infiltration Rate and ΔN_L; this excludes days in which vertical infiltration rates exceeded total infiltration rates; see section on Soils and Infiltration Rates for explanation. [c]Depth for field experiments indicates fluid samplers at the deepest piezometer (80 cm), while depth for laboratory experiments indicates samples collected from the column effluent. [d]Indicates single-tailed t test revealed significant difference ($p < 0.05$) between treatment (WC or BC) and control (NS) within the analysis period for either $[N]$ or ΔNL.

for *BC-Perc* and 0.7 ± 2.0 mg/L for *NS-Perc* (Table 1 and Figure 2C).

NS-Perc showed no consistent change with depth in either [DOC] or $[N]$ (Table S3, Figure 3A). In contrast, *WC-Perc* and *BC-Perc* showed significant changes with depth in both $[N]$ and [DOC]. *WC-Perc* showed $\Delta[N] = -3.6$ mg/L from the surface to the PRB and $\Delta[N] = -7.7$ mg/L from the surface to 30 cm bpb (Figures 2 and 3). [DOC] exhibited similar patterns with depth with the opposite sign: large Δ[DOC] within the PRB (4.5 mg/L) and at 30 cm bpb (8.0 mg/L relative to the surface; Figure 3B).

BC-Perc showed $\Delta[N] = -12.7$ mg/L and Δ[DOC] = 10.6 mg/L from the surface to PRB, indicating large nitrate removal within the PRB. However, these values showed opposite shifts below the PRB with $\Delta[N] = 6.0$ mg/L and Δ[DOC] = −6.4 mg/L from the PRB to 30 cm bpb (Figure 3C).

3.1.3. Stable Isotopes of NO_3. Nitrogen and oxygen stable isotopes showed a progressive enrichment with depth on days when nitrate removal was detected (Figures 3 and S8), suggesting that denitrification was a primary mechanism responsible for nitrate removal.[35,36] DNRA was likely not a significant pathway for NO_3 removal, as there was no pore fluid increase in $[NH_4^+]$ associated with lowered $[NO_3]$. Additionally, we observed no systematic increase in soil TN after any treatment or experiment, suggesting that $[NH_4^+]$ was not sorbed onto soil in measurable quantities (Figure S7). However, it remains possible that $[NH_4^+]$ was rapidly processed with little or no change to its standing stock; ongoing studies seek to identify potential nitrogen processing pathways using soil microbial transcriptomics.

We find average enrichment factors of $\varepsilon_N = -11.44‰$ and $\varepsilon_O = -8.32‰$, with a ratio of $\varepsilon_N/\varepsilon_O$ 1.38 for *WC-Perc*, and an average $\varepsilon_N = -4.83‰$ and $\varepsilon_O = -3.63‰$ with a ratio of $\varepsilon_N/\varepsilon_O$ 1.33 for *BC-Perc*. $\varepsilon_N/\varepsilon_O$ ratios reported elsewhere for bacterial denitrification range from 0.9 to 2.1.[37,38] Commonly reported ε_N values for field studies of microbial denitrification range from −4 to −30‰,[39,40] and results in the present study fall near the less negative end of this range. Relatively fewer ε_O factors have been reported in the literature, but ε_O factors from this study (−8.32 and −3.63‰) are broadly consistent with reported values for denitrification of −2 to −18‰.[37,41]

3.2. Lab Studies. *3.2.1. Soils and Infiltration Rate.* Sediments collected for laboratory column experiments showed a similar grain size distribution to those from the percolation tests *NS-Perc* and *WC-Perc* (Figure S5). Similarly, initial soil TOC and TN values in the soil columns were consistent with field samples (Figures S6 and S7).

Infiltration rates were 0.17, 0.18, and 0.18 m/day for the three columns during AP1 (Table 1 and Figure S4), overlapping with IR_V during field experiments (Figure 2A). Infiltration rates were raised to 0.70−0.74 m/day during AP2 (Table 1), similar to values that were found to enhance denitrification during earlier measurements in an active MAR system.[4]

3.2.2. Nutrient Changes. Influent water for all laboratory studies were drawn from the same source, although the composition varied somewhat when the 550-L supply tank had to be refilled. Surface $[N]$ and [DOC] were generally higher than those observed in the field. $\Delta[N]$ values during AP1 exhibited similar patterns to those measured in the field, with *NS-Col* showing less N removal than *WC-Col* or *BC-Col* (Table 1, Table S1, Figure S9). [DOC] also exhibited similar patterns to those observed in the field, with higher [DOC] following

DOI: 10.1021/acs.est.9b01191
Environ. Sci. Technol. 2019, 53, 9491−9501

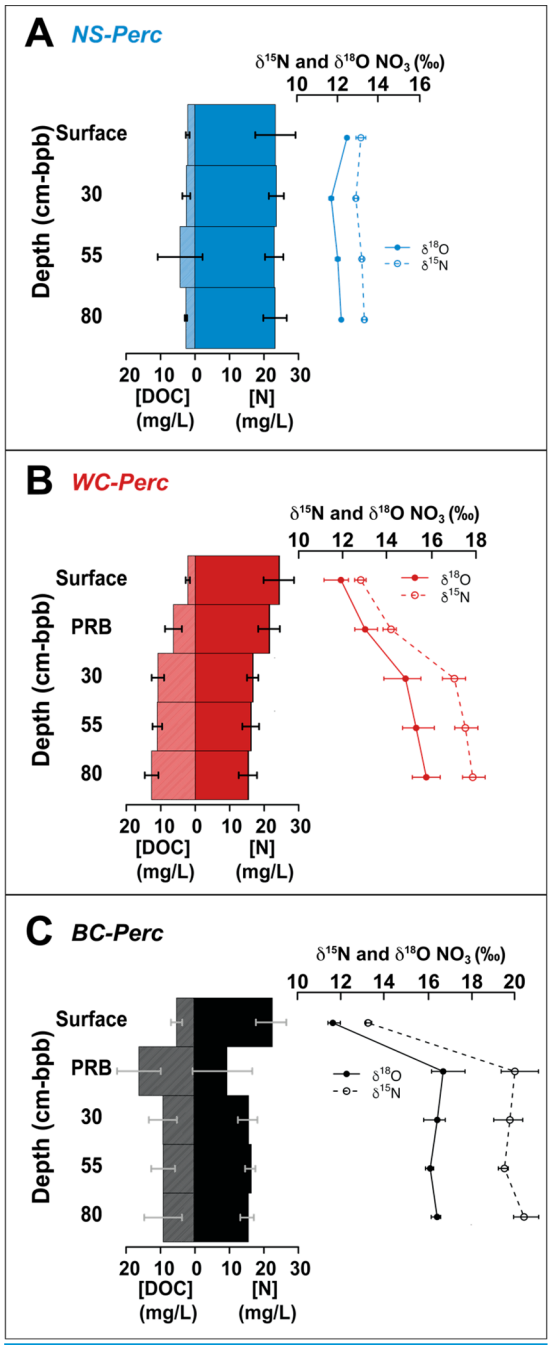

Figure 3. Average nutrient concentrations during the analysis period of field percolation experiments at measured depths show considerable differences between each soil treatment in [DOC], [*N*] and residual NO_3 $\delta^{15}N$ and $\delta^{18}O$. Increases in [DOC] are shown on the left of the bar plot, and increases to [*N*] are shown on the right of the bar plot. Bars show the range of nutrient and isotope measurements during the analysis period. (A) *NS-Perc* showed negligible changes with depth ([*N*] and [DOC], $p > 0.05$). Changes in [*N*] and [DOC] with depth are significant for *WC-Perc* and *BC-Perc* (single factor ANOVA, $p < 0.05$) but are insignificant for *NS-Perc* (Table S3). (B) During *WC-Perc*, there was a progressive decrease in [*N*] and increase in [DOC] both within and below the PRB and a fractionation in both $\delta^{15}N$ and $\delta^{18}O$ ([*N*] and [DOC], $p < 0.05$). (C) *BC-Perc* showed a decrease in [*N*] and increase in [DOC] within the PRB accompanied by an enrichment in $\delta^{15}N$ and $\delta^{18}O$, followed by a decrease in [DOC] and an increase in [*N*] with no isotope fractionation below the PRB ([*N*] and [DOC], $p < 0.05$).

passage through the woodchip/biochar PRBs and no consistent change in [DOC] during passage through the sand or native soil.

For *WC-Col* and *BC-Col*, higher infiltration rates during AP2 led to less N removal (lower magnitude $\Delta[N]$) than at lower infiltration rates during AP1 (Table S2). However, $\Delta[N]$ values were more similar during AP1 and AP2 for *NS-Col* (Figure 4).

3.3. Microbiological Changes. Groups of microorganisms that are thought to contribute to soil nitrogen and carbon cycling were found in both field and lab samples, including the Nitrospira family, capable of nitrite reduction,[42] and *Azoacorus*, a denitrifier which has been isolated from activated sludge.[43] Additionally, all sample groups included ammonia-oxidizing archaea of the phylum Thaumarchaeota[44] with a relative abundance of 3−5%. *Marmoricola*, within the order Propionibacteriales showed increases in relative abundance after *WC-Perc*, *BC-Perc*, *NS-Col*, and *BC-Col*; they are capable of reducing NO_3 using acetic acid and propionoic acid as carbon sources.[45] Small increases in the Sphingomonadaceae family, which contain species known to reduce nitrate[46] and utilize a wide variety of C sources,[47] were observed after *BC-Perc* and *BC-Col*.

Comparison of grouped soil samples before and after each test revealed no systematic shifts in the relative abundance of the most common phyla (Figure S10). This result contrasts distinctly with results from an earlier study in sandy soils,[25] where there were significant shifts in microbial ecology following infiltration. However, beta (between-sample) diversity plots for the current experiments show weak grouping of *WC-Perc* and *BC-Perc* compared to samples collected before the field studies began (Figure 4B). No such grouping was evident with samples collected from the laboratory studies.

4. DISCUSSION

4.1. Effect of PRB on Denitrification during Infiltration. In the field studies, both *WC-Perc* and *BC-Perc* showed statistically significant increases in [DOC] and decreases in [*N*], whereas *NS-Perc* showed no change with depth in either [DOC] or [*N*] (Table S3). Although both biochar and woodchips were associated with enhanced nitrate removal, their mechanisms for doing so appear to be different. It is generally understood that woodchips enhance denitrification through the release of organic carbon,[19,20,22,25] a portion of which is available for capable microbial communities to utilize as an electron donor for cellular processes. This increases rates of microbial respiration, which depletes oxygen concentrations, leading to the consumption of nitrate.

During *WC-Perc*, there was an increase in [DOC] within the PRB and a concomitant decrease in [*N*] (Figure 3B), accompanied by a fractionation of the residual NO_3 pool to values more enriched in $\delta^{15}N$ and $\delta^{18}O$ in a ratio indicative of denitrification (Figures 3B and S8). Additionally, these patterns continued below the PRB, at 30 cm bpb, where additional [DOC] increases were observed, along with even greater nitrogen removal and isotopic fractionation. These patterns persisted to depths of 55 and 80 cm bpb, although differences were smaller at depth (Figure 3B). These trends suggest that woodchips provide benefits by enhancing denitrification within the PRB, and those benefits are carried into the underlying soil by the infiltrating water, in effect extending the thickness of the zone where enhanced nitrogen processing can occur. These results are consistent with tests

DOI: 10.1021/acs.est.9b01191
Environ. Sci. Technol. 2019, 53, 9491−9501

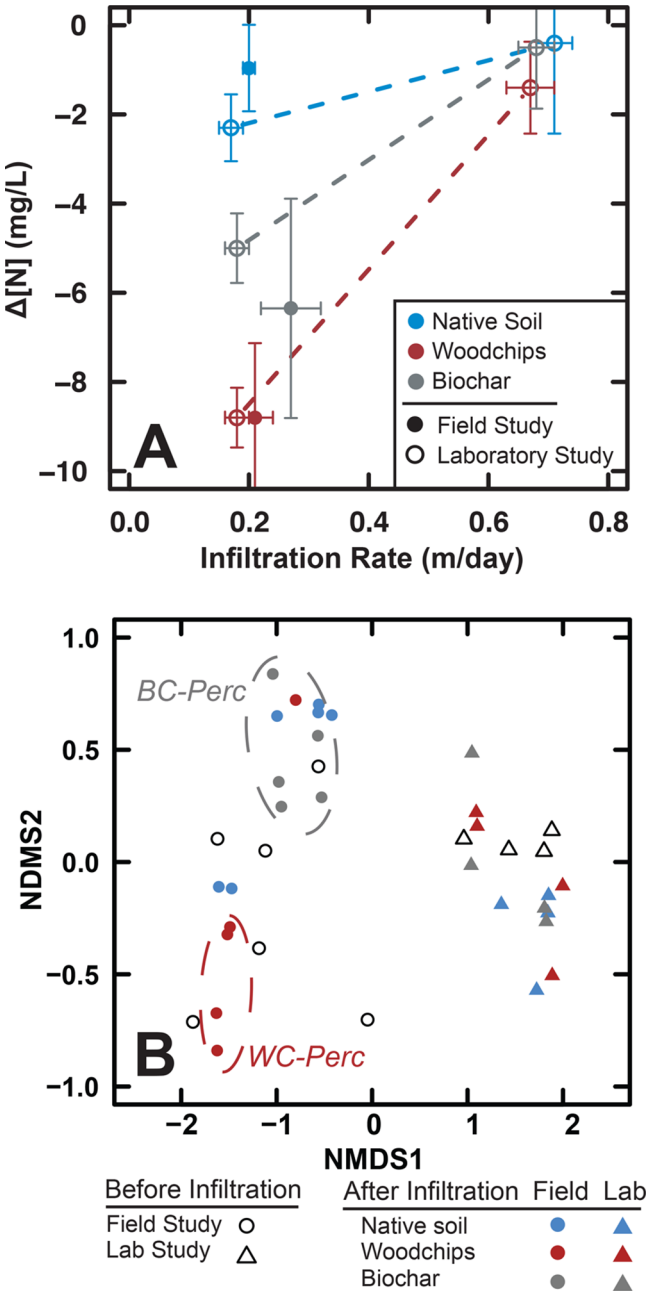

Figure 4. Combination of laboratory and field studies. (A) $\Delta[N]$ measurements across a range of vertical infiltration rates for field studies (closed circles) and laboratory studies (open circles) show that both woodchips and biochar are associated with greater magnitude $\Delta[N]$ at lower infiltration rates compared to higher infiltration rates during both field and laboratory testing. Additionally, both woodchips and biochar show greater magnitude $\Delta[N]$ compared to native soil treatments at lower infiltration rates (Tables 1, S1, and S2), but the difference is not significant at higher infiltration rates. Error bars show one standard deviation. (B) Beta (between sample) diversity of soil microbial community from before (open shapes) and after (closed shapes) each experiment, shows a weak grouping of *WC-Perc* and *BC-Perc* samples (red and gray closed circles). No such grouping is apparent for *NS-Perc* (blue closed circles) or laboratory studies (triangles). Beta diversity was calculated using Bray−Curtis distances with nonmetric multidimensional scaling (NMDS) for ordination (see SI, Section S1.6 for more detail).

done in coarser soils, which show denitrification occurring both within and below a woodchip PRB during rapid infiltration.[24]

In contrast, biochar appears to promote denitrification *within* but not *below* the PRB. During *BC-Perc*, we observed a large increase in [DOC] within the PRB associated with a large decrease in $[N]$ and an enrichment of residual NO_3 $\delta^{15}N$ and $\delta^{18}O$ (Figure 3C), all consistent with denitrification. However, below the PRB, $[N]$ increased and [DOC] decreased, with no fractionation of residual NO_3 isotopes (Figure 3C). These $[N]$ increases below the PRB could be associated with physical processes such as absorption/desorption, which do not appreciably fractionate stable isotopes,[48,49] suggesting that some of the $[N]$ removal that occurred within the biochar PRB was reversible.

Biochar can affect soil N and C cycling through many mechanisms;[48,49] for example, its high specific surface area[50] has been shown to provide an abundance of locations for microbial communities to colonize, which could help to explain high rates of cycling within the PRB (resulting in NO_3 isotopic shifts) that are not continued within the underlying soil.

4.2. Effect of Infiltration Rate on Denitrification during Infiltration. The effect of infiltration rate on denitrification is best elucidated by comparing AP1 and AP2 during laboratory columns studies, where the infiltration rate was more easily controlled. All three treatments showed higher magnitude $\Delta[N]$ (more N removal) at lower infiltration rates (Tables 1 and S2). These results are consistent with the understanding that higher infiltration rates result in greater penetration of oxygen and less favorable conditions for denitrification. Previous studies have identified fluid residence time as a primary control on nitrogen removal within bioreactor systems,[27,51,52] but conditions in those systems are fundamentally different from those that occur during infiltration for MAR. In particular, residence times under saturated conditions during the present study are shorter and less easily controlled than those commonly seen in bioreactors. In addition, the present study shows that the infiltration rate dependence of denitrification is influenced by the presence and type of a PRB carbon source.

Figure 4A shows the relationship between $\Delta[N]$ and infiltration rate, demonstrating that both biochar and woodchip PRBs significantly enhanced denitrification at lower infiltration rates. At higher infiltration rates, the biochar and woodchips had no discernible effects compared to the native soil (Table S1). Distinct relationships between $\Delta[N]$ and infiltration rate are suggested based on the presence and composition of a PRB (Figure 4A), but additional work will be needed to assess the monotonic (possibly nonlinear) nature of these relations.

The consistently low ΔN_L values for the NS experiments across all infiltration rates (Table 1, Figure S9) are comparable to measurements of denitrification during controlled percolation studies and active MAR operations ($\Delta N_L \sim 0.20$ g-N/day·m^{-2}) in coarser-grained soils.[4,24] For WC and BC treatments, lower infiltration rates are associated with higher magnitude ΔN_L (more N load reduction) at higher infiltration rates (Table 1, Figure S9). This dependence appears to be similar to that for $\Delta[N]$; because ΔN_L is the product of $\Delta[N]$ and infiltration rate, ΔN_L values are neither maximized at low infiltration rates nor at high infiltration rates (due to low $\Delta[N]$). Instead, there is likely an intermediate range of

DOI: 10.1021/acs.est.9b01191
Environ. Sci. Technol. 2019, 53, 9491−9501

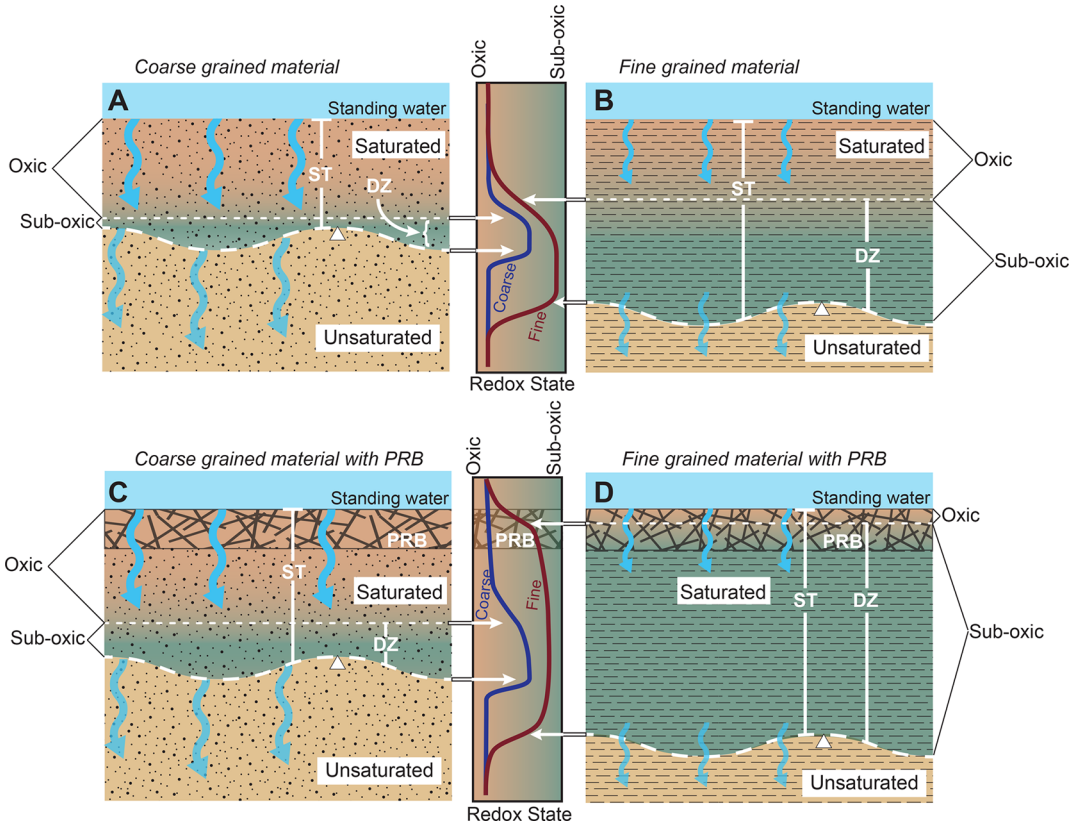

Figure 5. Schematic representation of primary factors controlling denitrification during infiltration through coarse-grained soil (A and C) and fine-grained soil (B and D) with (parts C and D) and without (parts A and B) a woodchip PRB. Patterns are generalized based on results from this study and similar studies done in coarser-grained soils[24], showing the relative saturated thickness (ST) and the denitrification zone (DZ). Central plots show generic curves illustrating depth profiles of the relative redox conditions for coarse- (blue) and fine-grained (red) soils. Oxic conditions favor O_2 as the primary e- acceptor, whereas suboxic to reducing conditions are more favorable to NO_3. Orange areas indicate oxic zones in which denitrification is not favored, and green areas indicate suboxic (reducing) conditions under which denitrification is favored.

infiltration rates that result in maximum ΔN_L, as a function of the nature of the carbon source, soil properties, and other factors. As ΔN_L is of primary concern for the health of aquifers and surface water bodies through the reduction of export loads, our results suggest it may be possible to identify an optimum infiltration rate for a given set of MAR conditions.

4.3. Effect of Infiltration on Microbial Ecology. Observed nitrate load reduction during biochar and woodchip PRB field and laboratory experiments, coupled with relatively modest changes in the diversity and relative abundance of soil microbial communities before and after each test, suggest that sufficient microorganisms capable of carrying out denitrification during infiltration were present in the soil before the start of infiltration. The change in $[N]$ (and ΔN_L) is likely the result of these preexisting microorganisms increasing their activity in response to changes in environmental conditions (i.e., water saturation, availability of carbon, development of suboxic/anoxic conditions). The presence of microorganisms that have previously been identified as important in nitrogen and carbon cycling in soils is consistent with this interpretation. Sphingomonadaceae, a family with many genera capable of nitrate reduction,[46] was observed in all samples. Other researchers have observed increases in its relative abundance in the presence of woodchips[24] and biochar,[53] and have interpreted those increases as a signal of the family's importance to soil nitrogen and carbon cycling. Similarly, the order Burkholderiales and family Bradyrhizobiaceae were present in all sample groups and have been identified as potentially important groups carrying out key steps of denitrification in both amended[47] and unamended[54] soils.

The immense complexity and interconnectedness of soil microbial ecology make it unlikely that changes in nutrient cycling can be directly connected to changes in individual groups of microorganisms without more detailed investigations, including studies focused on functional activity and soil metagenomics and metatranscriptomics. Additional work is underway that explores these topics and should help to elucidate microbial controls on denitrification (and nutrient cycling more broadly) during infiltration for MAR.

4.4. Physical and Chemical Controls on Denitrification during Infiltration. By combining the results from the current study with similar studies carried out in coarse-grained soil,[4,25] we developed a conceptual model that illustrates how two primary factors may affect denitrification during infiltration: (1) the presence or absence of a bioavailable carbon source and (2) soil texture and associated influences on pore fluid storage and flow rate (Figure 5).

The effect of the woodchip PRB (Figure 5C,D) is 2-fold; first, the PRB supplies carbon (and potentially habitat and/or other benefits) to microbial communities that have the capacity to accomplish denitrification. Second, the PRB affects the thickness of the saturated zone that develops in the shallow soil above an inverted water table during infiltration. Considerable geochemical processing occurs within this zone, including denitrification, under suitable conditions. The addition of a PRB increases the thickness of the saturated

DOI: 10.1021/acs.est.9b01191
Environ. Sci. Technol. 2019, 53, 9491−9501

zone without having a significant impact on the infiltration rate, because PRB materials tend to have large particle sizes relative to the underlying native soil. The increased saturated thickness, in turn, increases the residence time of fluid within this zone.

The second factor, soil texture, has a primary influence on both the infiltration rate and the saturated zone thickness. Coarser soils tend to have higher infiltration rates than finer soils, resulting in a lower residence time for a given saturated thickness. But in addition, coarser soils tend to also be better drained, leading to a shallower inverted water table. We did not measure the saturated thickness during field percolation tests in the present study but have found that shallow piezometers tend to produce fluid samples at greater depths in finer-grained soils than in coarser-grained soils (SI Section S2.2 and Figure S11), a trend consistent with other field studies.[4,25] Thus fluids infiltrating coarser soils tend to have a shorter residence time within the saturated zone compared to that in finer soils, both because the infiltration rate is greater and because the saturated zone is thinner.

We hypothesize that these two processes will tend to reinforce differences in conditions that are most favorable for denitrification (Figure 5). Oxygen infiltrating with surface water into shallow soils can reach the base of the saturated zone if the fluid is moving too quickly for soil microbes to consume it and/or because the saturated zone is thin. Both conditions are more likely to occur in coarse soils than in fine soils. In finer soils, the saturated zone is likely to be thicker to begin with, compared to that in coarser soils, and the slower rate of infiltration tends to result in a commensurately longer fluid residence time in the saturated zone and thus conditions that are more favorable for denitrification. Adding a carbon-rich PRB makes denitrification more favorable for both coarse and fine soils (Figure 5) by helping to speed the rate of biological consumption of available oxygen, but the extent to which this favorability is expressed depends on the details of saturated zone thickness and infiltration rate (and thus residence time), the concentration of nitrate, and the bioavailability of carbon.

Both woodchips and biochar demonstrate potential to enhance nitrate removal during infiltration, but $[N]$ processing in shallow soils below a woodchip PRB is more clearly associated in the present study with denitrification. In contrast, while a biochar PRB may also provide a sink for nitrate, some of the $\Delta[N]$ apparent from field and laboratory tests with biochar may have resulted from absorption or denitrification that occurs mainly within the PRB layer. It may be that a PRB assembled from a mixture of woodchips and biochar would be particularly beneficial, as it could both slow the movement of nitrate by adsorption and provide habitat for microbial consortia that accomplish denitrification (among other functions).

Our results, in combination with other studies, suggest that infiltration for managed recharge could be optimized for improvements to both water supply and water quality. Given the long-term challenges in many basins associated with managing loads of salts and nutrients, there may be benefits to designing MAR systems to provide opportunities to improve water quality, not just avoid degradation. Many questions remain about the complex interplay between physical and chemical conditions and processes that could stimulate naturally occurring microbiological communities in the subsurface to consume and process carbon and nutrients during MAR. While each infiltration and recharge project is subject to specific goals and conditions and a variety of water quality concerns involving redox-sensitive solutes, the definition of quantitative links between biogeochemical cycling and physical hydrologic processes can lead to improved practices, helping to enhance resources under a range of natural and managed conditions.

■ ASSOCIATED CONTENT

Supporting Information

The Supporting Information is available free of charge on the ACS Publications website at DOI: 10.1021/acs.est.9b01191.

Detailed description of experimental methods and design, analytical techniques (PDF)

Tabulated pore water chemistry data for all experiments (XLSX)

Tabulated OTU assignments for all soil samples analyzed (XLSX)

■ AUTHOR INFORMATION

Corresponding Author

*E-mail: ggorski@ucsc.edu.

ORCID

Galen Gorski: 0000-0003-0083-4251

Andrew T Fisher: 0000-0003-2102-8320

Present Addresses

[#]Department of Earth and Environmental Science, Temple University, Philadelphia, PA 19122, U.S.A.

[$]Desert Research Institute, Reno, NV 89514, U.S.A.

[⊥]Department of Ecology and Evolutionary Biology, University of California Irvine, Irvine, CA 92697, U.S.A.

Funding

This project was supported by the Gordon and Betty Moore Foundation (Grant GBMF5595), UC Water Security and Sustainability Research Initiative (UCOP Grant # 13941), the USDA/NIFA (Award #2017−67026−26315), the Water Foundation (Award #10069), the National Science Foundation Graduate Research Fellowship Program, and the Recharge Initiative (http://www.rechargeinitiative.org/).

Notes

The authors declare no competing financial interest.

■ ACKNOWLEDGMENTS

We gratefully acknowledge the laboratory and field assistance of A. Paytan, R. Franks, D. Sampson, H. Dailey, E. Adelstein, T. Weathers, P. Karim, M. Cribari, D. van den Dries, T. Stewart, A. Yoder, K. Young, J. Cox, A. Serrano, and J. Pensky. We would like to thank E. and J. Kelly, S. Dobbler, T. Marg, K. Camara, C. Coburn, and B. Lockwood for their key guidance and cooperation on conducting the field studies.

■ ABBREVIATIONS

MAR	managed aquifer recharge
PRB	permeable reactive barrier
bpb	below plot base
NS	native soil
WC	woodchips
BC	biochar
DOC	dissolved organic carbon
OTU	operational taxonomic unit
DNRA	dissimilatory nitrate reduction to ammonia

DOI: 10.1021/acs.est.9b01191
Environ. Sci. Technol. 2019, 53, 9491−9501

ST saturated thickness
DZ denitrification zone

REFERENCES

(1) Wada, Y.; Van Beek, L. P. H.; Van Kempen, C. M.; Reckman, J. W. T. M.; Vasak, S.; Bierkens, M. F. P. Global Depletion of Groundwater Resources. *Geophys. Res. Lett.* **2010**, *37* (20), 1−5.

(2) Bouwer, H. Artificial Recharge of Groundwater: Hydrogeology and Engineering. *Hydrogeol. J.* **2002**, *10* (1), 121−142.

(3) Beganskas, S.; Fisher, A. T. Coupling Distributed Stormwater Collection and Managed Aquifer Recharge: Field Application and Implications. *J. Environ. Manage.* **2017**, *200*, 366−379.

(4) Schmidt, C. M.; Fisher, A. T.; Racz, A. J.; Lockwood, B. S.; Huertos, M. L. Linking Denitrification and Infiltration Rates during Managed Groundwater Recharge. *Environ. Sci. Technol.* **2011**, *45* (22), 9634−9640.

(5) Grau-Martínez, A.; Folch, A.; Torrentó, C.; Valhondo, C.; Barba, C.; Domènech, C.; Soler, A.; Otero, N. Monitoring Induced Denitrification during Managed Aquifer Recharge in an Infiltration Pond. *J. Hydrol.* **2018**, *561*, 123−135.

(6) Bekele, E.; Toze, S.; Patterson, B.; Higginson, S. Managed Aquifer Recharge of Treated Wastewater: Water Quality Changes Resulting from Infiltration through the Vadose Zone. *Water Res.* **2011**, *45* (17), 5764−5772.

(7) Ganot, Y.; Holtzman, R.; Weisbrod, N.; Russak, A.; Katz, Y.; Kurtzman, D. Geochemical Processes During Managed Aquifer Recharge With Desalinated Seawater. *Water Resour. Res.* **2018**, *54* (2), 978−994.

(8) Dallman, S.; Spongberg, M. Expanding Local Water Supplies: Assessing the Impacts of Stormwater Infiltration on Groundwater Quality. *Prof. Geogr.* **2012**, *64* (2), 232−249.

(9) Groffman, P. M.; Altabet, M. A.; Bohlke, J. K.; Butterbach-Bahl, K.; David, M. B.; Firestone, M. K.; Giblin, A. E.; Kana, T. M.; Nielsen, L. P.; Voytek, M. A. Methods for Measuring Denitrification. *Ecol. Appl.* **2006**, *16*, 2091−2122.

(10) Tedoldi, D.; Chebbo, G.; Pierlot, D.; Kovacs, Y.; Gromaire, M. C. Impact of Runoff Infiltration on Contaminant Accumulation and Transport in the Soil/Filter Media of Sustainable Urban Drainage Systems: A Literature Review. *Sci. Total Environ.* **2016**, *569−570*, 904−926.

(11) Burow, K. R.; Nolan, B. T.; Rupert, M. G.; Dubrovsky, N. M. Nitrate in Groundwater of the United States, 1991−2003. *Environ. Sci. Technol.* **2010**, *44* (13), 4988−4997.

(12) Kaushal, S. S.; Groffman, P. M.; Band, L. E.; Elliott, E. M.; Shields, C. A.; Kendall, C. Tracking Nonpoint Source Nitrogen Pollution in Human-Impacted Watersheds. *Environ. Sci. Technol.* **2011**, *45*, 8225−8232.

(13) Carpenter, A. S. R.; Caraco, N. F.; Correll, D. L.; Howarth, R. W.; Sharpley, A. N.; Smith, V. H. Nonpoint Pollution of Surface Waters with Phophorous and Nitrogen. *Ecol. Appl.* **1998**, *8* (3), 559−568.

(14) Gurdak, J. J.; Qi, L. Vulnerability of Recently Recharged Groundwater in the High Plains Aquifer To Nitrate Contamination. *Sci. Invest. Rep.* **2006**, *36*, 6004−6012.

(15) Vitousek, P. M.; Aber, J. D.; Howarth, R. W.; Likens, G. E.; Matson, A.; Schindler, D. W.; Schlesinger, W. H.; Tilman, D. G. Human Alteration of the Global Nitrogen Cycle: Sources and Consequences. *Ecol. Appl.* **1997**, *7* (3), 737−750.

(16) Korom, S. F. Natural Denitrification in the Saturated Zone: A Review. *Water Resour. Res.* **1992**, *28* (6), 1657−1668.

(17) Seitzinger, S.; Harrison, J. A.; Bohlke, J. K.; Bouwman, A. F.; Lowrance, R.; Peterson, B.; Tobias, C.; Drecht, G. V. Denitrification Across Landscapes and Waterscapes: A Synthesis. *Ecol. Appl.* **2006**, *16* (6), 2064−2090.

(18) Bock, E.; Smith, N.; Rogers, M.; Coleman, B.; Reiter, M.; Benham, B.; Easton, Z. M. Enhanced Nitrate and Phosphate Removal in a Denitrifying Bioreactor with Biochar. *J. Environ. Qual.* **2015**, *44* (2), 605.

(19) Schipper, L. A.; Vojvodić-Vuković, M. Five Years of Nitrate Removal, Denitrification and Carbon Dynamics in a Denitrification Wall. *Water Res.* **2001**, *35* (14), 3473−3477.

(20) Robertson, W. D.; Merkley, L. C. In-Stream Bioreactor for Agricultural Nitrate Treatment. *J. Environ. Qual.* **2009**, *38*, 230−238.

(21) Christianson, L. E.; Lepine, C.; Sharrer, K. L.; Summerfelt, S. T. Denitrifying Bioreactor Clogging Potential during Wastewater Treatment. *Water Res.* **2016**, *105*, 147−156.

(22) Schipper, L. A.; Barkle, G. A.; Vojvodić-Vuković, M. Maximum Rates of Nitrate Removal in a Denitrification Wall. *J. Environ. Qual.* **2005**, *34* (4), 1270−1276.

(23) Schipper, L. A.; Robertson, W. D.; Gold, A. J.; Jaynes, D. B.; Cameron, S. C. Denitrifying Bioreactors - An Approach for Reducing Nitrate Loads to Receiving Waters. *Ecol. Eng.* **2010**, *36* (11), 1532−1543.

(24) Beganskas, S.; Gorski, G.; Weathers, T.; Fisher, A. T.; Schmidt, C.; Saltikov, C.; Redford, K.; Stoneburner, B.; Harmon, R.; Weir, W. A Horizontal Permeable Reactive Barrier Stimulates Nitrate Removal and Shifts Microbial Ecology during Rapid Infiltration for Managed Recharge. *Water Res.* **2018**, *144*, 274−284.

(25) Beganskas, S.; Young, K. S.; Fisher, A. T.; Harmon, R.; Lozano, S. Runoff Modeling of a Coastal Basin to Assess Variations in Response to Shifting Climate and Land Use: Implications for Managed Recharge. *Water Resour. Manag.* **2019**, *33*, 1683.

(26) Hatch, C. E.; Fisher, A. T.; Revenaugh, J. S.; Constantz, J.; Ruehl, C. Quantifying Surface Water-Groundwater Interactions Using Time Series Analysis of Streambed Thermal Records: Method Development. *Water Resour. Res.* **2006**, *42* (10), 1−14.

(27) Halaburka, B. J.; Lefevre, G. H.; Luthy, R. G. Evaluation of Mechanistic Models for Nitrate Removal in Woodchip Bioreactors. *Environ. Sci. Technol.* **2017**, *51* (9), 5156−5164.

(28) Moon, H. S.; Shin, D. Y.; Nam, K.; Kim, J. Y. A Long-Term Performance Test on an Autotrophic Denitrification Column for Application as a Permeable Reactive Barrier. *Chemosphere* **2008**, *73* (5), 723−728.

(29) Della Rocca, C.; Belgiorno, V.; Meriç, S. An Heterotrophic/Autotrophic Denitrification (HAD) Approach for Nitrate Removal from Drinking Water. *Process Biochem.* **2006**, *41* (5), 1022−1028.

(30) Gibert, O.; Pomierny, S.; Rowe, I.; Kalin, R. M. Selection of Organic Substrates as Potential Reactive Materials for Use in a Denitrification Permeable Reactive Barrier (PRB). *Bioresour. Technol.* **2008**, *99*, 7587−7596.

(31) Healy, M. G.; Ibrahim, T. G.; Lanigan, G. J.; Serrenho, A. J.; Fenton, O. Nitrate Removal Rate, Efficiency and Pollution Swapping Potential of Different Organic Carbon Media in Laboratory Denitrification Bioreactors. *Ecol. Eng.* **2012**, *40*, 198−209.

(32) Klindworth, A.; Pruesse, E.; Schweer, T.; Peplies, J.; Quast, C.; Horn, M.; Glöckner, F. O. Evaluation of General 16S Ribosomal RNA Gene PCR Primers for Classical and Next-Generation Sequencing-Based Diversity Studies. *Nucleic Acids Res.* **2013**, *41* (1), 1−11.

(33) Racz, A. J.; Fisher, A. T.; Schmidt, C. M.; Lockwood, B. S.; Huertos, M. L. Spatial and Temporal Infiltration Dynamics During Managed Aquifer Recharge. *Groundwater* **2012**, *50* (4), 562−570.

(34) Clark, J. F.; Hudson, G. B.; Davisson, M. L.; Woodside, G.; Herndon, R. Geochemical Imaging of Flow Near an Artificial Recharge Facility, Orange County, California. *Groundwater* **2004**, *42* (2), 167−174.

(35) Mariotti, A.; Landreau, A.; Simon, B. 15N Isotope Biogeochemistry and Natural Denitrification Process in Groundwater: Application to the Chalk Aquifer of Northern France. *Geochim. Cosmochim. Acta* **1988**, *52* (7), 1869−1878.

(36) Kendall, C.; Caldwell, E.. *Isotope Tracers in Catchment Hydrology*; Kendall, C., McDonnell, J. J., Eds.; Elsevier: Amsterdam, 1998.

(37) Otero, N.; Torrentó, C.; Soler, A.; Menció, A.; Mas-Pla, J. Monitoring Groundwater Nitrate Attenuation in a Regional System Coupling Hydrogeology with Multi-Isotopic Methods: The Case of Plana de Vic (Osona, Spain). *Agric., Ecosyst. Environ.* **2009**, *133* (1−2), 103−113.

DOI: 10.1021/acs.est.9b01191
Environ. Sci. Technol. 2019, 53, 9491−9501

(38) Bottcher, J.; Strebel, O.; Voerkelius, S.; Schmidt, H.-L. Using Isotope Fractionation of Nitrate-Nitrogen and Nitrate-Oxygen for Evaluation of Microbial Denitrification in a Sandy Aquifer. *J. Hydrol.* **1990**, *114*, 413−424.
(39) Vogel, J. C.; Talma, A. S.; Heaton, T. H. E. Gaseous Nitrogen as Evidence for Denitrification in Groundwater. *J. Hydrol.* **1981**, *50* (C), 191−200.
(40) Pauwels, H.; Foucher, J. C.; Kloppmann, W. Denitrification and Mixing in a Schist Aquifer: Influence on Water Chemistry and Isotopes. *Chem. Geol.* **2000**, *168* (3−4), 307−324.
(41) Mengis, M.; Schif, S. L.; Harris, M.; English, M. C.; Aravena, R.; Elgood, R. J.; MacLean, A. Multiple Geochemical and Isotopic Approaches for Assessing Ground Water NO3- Elimination in a Riparian Zone. *Groundwater* **1999**, *37*, 448−457.
(42) Koch, H.; Lücker, S.; Albertsen, M.; Kitzinger, K.; Herbold, C.; Spieck, E.; Nielsen, P. H.; Wagner, M.; Daims, H. Expanded Metabolic Versatility of Ubiquitous Nitrite-Oxidizing Bacteria from the Genus *Nitrospira*. *Proc. Natl. Acad. Sci. U. S. A.* **2015**, *112* (36), 11371−11376.
(43) Hagman, M.; Nielsen, J. L.; Nielsen, P. H.; Jansen, J. C. Mixed Carbon Sources for Nitrate Reduction in Activated Sludge-Identification of Bacteria and Process Activity Studies. *Water Res.* **2008**, *42*, 1539−1546.
(44) Spang, A.; Poehlein, A.; Offre, P.; Zumbrägel, S.; Haider, S.; Rychlik, N.; Nowka, B.; Schmeisser, C.; Lebedeva, E. V.; Rattei, T.; Bohm, C.; Schmid, M.; Galushko, A.; Hatzenpichler, R.; Weinmaier, T.; Daniel, R.; Schleper, C.; Spieck, E.; Streit, W.; Wagner, M. The Genome of the Ammonia-Oxidizing Candidatus Nitrososphaera Gargensis: Insights into Metabolic Versatility and Environmental Adaptations. *Environ. Microbiol.* **2012**, *14* (12), 3122−3145.
(45) Dastager, S. G.; Lee, J. C.; Ju, Y. J.; Park, D. J.; Kim, C. J. Marmoricola Bigeumensis Sp. Nov., a Member of the Family Nocardioidaceae. *Int. J. Syst. Evol. Microbiol.* **2008**, *58* (5), 1060−1063.
(46) Takeuchi, M.; Hamana, K.; Hiraishi, A. Proposal of the Genus Sphingomonas Sensu Stricto and Three New Genera. *Int. J. Syst. Evol. Microbiol.* **2001**, *51* (4), 1405−1417.
(47) Anderson, C. R.; Condron, L. M.; Clough, T. J.; Fiers, M.; Stewart, A.; Hill, R. A.; Sherlock, R. R. Biochar Induced Soil Microbial Community Change: Implications for Biogeochemical Cycling of Carbon, Nitrogen and Phosphorus. *Pedobiologia* **2011**, *54* (5−6), 309−320.
(48) Clough, T. J.; Condron, L. M. Biochar and the Nitrogen Cycle: Introduction. *J. Environ. Qual.* **2010**, *39* (4), 1218.
(49) Kameyama, K.; Miyamoto, T.; Shiono, T.; Shinogi, Y. Influence of Sugarcane Bagasse-Derived Biochar Application on Nitrate Leaching in Calcaric Dark Red Soil. *J. Environ. Qual.* **2012**, *41* (4), 1131.
(50) Atkinson, C. J.; Fitzgerald, J. D.; Hipps, N. A. Potential Mechanisms for Achieving Agricultural Benefits from Biochar Application to Temperate Soils: A Review. *Plant Soil* **2010**, *337* (1), 1−18.
(51) Greenan, C. M.; Moorman, T. B.; Parkin, T. B.; Kaspar, T. C.; Jaynes, D. B. Denitrification in Wood Chip Bioreactors at Different Water Flows. *J. Environ. Qual.* **2009**, *38* (4), 1664−1671.
(52) Hoover, N. L.; Bhandari, A.; Soupir, M. L.; Moorman, T. B. Woodchip Denitrification Bioreactors: Impact of Temperature and Hydraulic Retention Time on Nitrate Removal. *J. Environ. Qual.* **2016**, *45* (3), 803−812.
(53) Xu, H.-J.; Wang, X.-H.; Li, H.; Yao, H.-Y.; Su, J.-Q.; Zhu, Y.-G. Biochar Impacts Soil Microbial Community Composition and Nitrogen Cycling in an Acidic Soil Planted with Rape. *Environ. Sci. Technol.* **2014**, *17* (i), 9391−9399.
(54) Liu, Y.; Liu, C.; Nelson, W. C.; Shi, L.; Xu, F.; Liu, Y.; Yan, A.; Zhong, L.; Thompson, C.; Fredrickson, J. K.; Zachara, J. M. Effect of Water Chemistry and Hydrodynamics on Nitrogen Transformation Activity and Microbial Community Functional Potential in Hyporheic Zone Sediment Columns. *Environ. Sci. Technol.* **2017**, *51* (9), 4877−4886.

DOI: 10.1021/acs.est.9b01191
Environ. Sci. Technol. 2019, 53, 9491−9501